Published in final edited form as:
Dev Biol. 2010 November 1; 347(1): 167–179. doi:10.1016/j.ydbio.2010.08.021.

Twist1 promotes heart valve cell proliferation and extracellular matrix gene expression during development in vivo and is expressed in human diseased aortic valves

Santanu Chakraborty[1], **Elaine E. Wirrig**[1], **Robert B. Hinton**[1], **Walter H. Merrill**[2,3], **Douglas B. Spicer**[4], and **Katherine E. Yutzey**[1,*]

[1]The Heart Institute, Cincinnati Children's Medical Center, Cincinnati, OH 45229

[2]Division of Cardiothoracic Surgery, University of Cincinnati, College of Medicine, Cincinnati, OH 45219

[4]Center for Molecular Medicine, Maine Medical Center Research Institute, Scarborough, ME 04074

Abstract

During embryogenesis the heart valves develop from undifferentiated mesenchymal endocardial cushions (EC), and activated interstitial cells of adult diseased valves share characteristics of embryonic valve progenitors. Twist1, a class II basic-helix-loop-helix (bHLH) transcription factor, is expressed during early EC development and is downregulated later during valve remodeling. The requirements for *Twist1* down-regulation in the remodeling valves and the consequences of prolonged Twist1 activity were examined in transgenic mice with persistent expression of Twist1 in developing and mature valves. Persistent Twist1 expression in the remodeling valves leads to increased valve cell proliferation, increased expression of Tbx20, and increased extracellular matrix (ECM) gene expression, characteristic of early valve progenitors. Among the ECM genes predominant in the EC, *Col2a1* was identified as a direct transcriptional target of Twist1. Increased Twist1 expression also leads to dysregulation of fibrillar collagen and periostin expression, as well as enlarged hypercellular valve leaflets prior to birth. In human diseased aortic valves, increased Twist1 expression and cell proliferation are observed adjacent to nodules of calcification. Overall, these data implicate Twist1 as a critical regulator of valve development and suggest that Twist1 influences ECM production and cell proliferation during disease.

Keywords

heart valve development; aortic valve disease; Twist1; bHLH transcription factor; extracellular matrix; cell proliferation

[*]Address Correspondence to: Katherine E. Yutzey Division of Molecular Cardiovascular Biology Cincinnati Children's Medical Center ML 7020 240 Albert Sabin Way Cincinnati, OH 45229 Tel: 513-636-8340; Fax: 513-636-5958, katherine.yutzey@cchmc.org.
[3]Present address: Division of Cardiothoracic Surgery, University of Mississippi, Jackson, MS 39216

Introduction

In the United States, 20–30% of all congenital cardiovascular malformations are associated with valve defects, and diseased valves requiring replacement often have congenital anomalies (Loffredo, 2000; Roberts and Ko, 2005). Heart valve development is characterized by the transition of highly proliferative undifferentiated progenitor cells of the endocardial cushions to quiescent valve interstitial cells (VIC) embedded in a complex stratified extracellular matrix (ECM) in the mature valves (Combs and Yutzey, 2009). Likewise, the initial stages of valve disease are characterized by activation of VICs, followed by increased production and disorganization of the valve ECM, leading to thickening of the valve leaflets (Hinton et al., 2006; Rabkin et al., 2001; Rabkin-Aikawa et al., 2004). Embryonic valve progenitor cells are characterized by cell proliferation, migration, and primitive ECM production, which are also characteristics of activated VICs in disease (Aikawa et al., 2006; Rabkin-Aikawa et al., 2004; Schoen, 2008). Several signaling pathways and transcription factors, including the bHLH factor Twist1, have been implicated in maintaining the valve progenitor phenotype during development based on cell culture studies (Shelton and Yutzey, 2008). However, the consequences of persistent expression of early endocardial cushion transcription factors during later stages of remodeling in vivo have not been previously demonstrated. Moreover, potential roles for regulators of valve progenitor cells in adult human valve pathogenesis or repair have not been reported.

The development of the heart valves initiates with the formation of endocardial cushions (EC) in the atrioventricular (AV) junction and outflow tract (OFT) of the primitive heart tube (Combs and Yutzey, 2009). Heart valve progenitor cells arise from an epithelial to mesenchymal transformation (EMT) and are a highly proliferative, migratory, and undifferentiated mesenchymal cell population within the EC. Heart valve remodeling during fetal and neonatal development is characterized by the reduced proliferation of progenitor cells with increased complexity and organization of stratified ECM in the semilunar (SL) and AV valve leaflets (Aikawa et al., 2006; Hinton et al., 2006). In addition, matrix metalloproteinases (MMPs) and ECM protein genes, including collagens 2 and 9 are preferentially expressed in EC, whereas fibrillar collagens 1 and 3 are predominant in the remodeling valves (Chakraborty et al., 2008). The mature AV and SL valve leaflets are stratified into elastin, proteoglycan, and collagen-rich ECM layers with VICs that exhibit little to no cell proliferation (Combs and Yutzey, 2009). The molecular and cellular mechanisms that govern the transition of proliferative, migratory, undifferentiated valve progenitor cells of the EC into the differentiated, relatively quiescent VICs of the mature valves are not well-characterized.

Twist1, a class II category basic-helix-loop-helix (bHLH) transcription factor, regulates morphogenesis in a variety of developing organ systems, including the heart, and also promotes EMT during development and in tumor metastasis (Barnes and Firulli, 2009; Yang et al., 2004). Twist1 haploinsufficiency in humans is associated with Saethre-Chotzen syndrome, characterized by craniofacial abnormalities, skeletal anomalies, and limb patterning defects (Reardon and Winter, 1994). During development, *Twist1* is highly expressed in EC, and its expression is down-regulated during heart valve remodeling (Chakraborty et al., 2008). In cultured avian embryonic EC, Twist1 promotes cell proliferation and migration, while inhibiting differentiation (Shelton and Yutzey, 2008). However, the requirements for *Twist1* down-regulation in the remodeling valves and the consequences of prolonged Twist1 activity in adult valves have not been determined previously.

In this study, transgenic mice with persistent Twist1 expression in remodeling and adult valves were generated in order to determine the effects of prolonged Twist1 expression on valvulogenesis. Increased Twist1 expression leads to increased cell proliferation, prolonged expression of endocardial cushion ECM proteins, and abnormal valve morphogenesis. In adult

human diseased valves, Twist1 expression is induced in regions of increased cell proliferation and ECM disorganization. Together these studies provide in vivo evidence for Twist1 function in heart valve development and disease.

Materials and methods

Generation of mice

Female *CAG-CAT-Twist1* mice (Connerney et al., 2006) were bred with *Tie2Cre* males (Kisanuki et al., 2001) (Jackson Laboratories, stock number: 004128) to generate double transgenic embryos, neonates, and adult offspring. Timed matings were established, with the morning of an observed copulation plug set at E0.5. All studies were performed on cohorts of *CAG-CAT-Twist1;Tie2Cre* double transgenic (DTG) animals compared to *CAG-CAT-Twist1* single transgenic (STG) littermate controls. *CAG-CAT-Twist1;Tie2Cre* DTG animals were obtained at expected Mendelian ratios, and no embryonic or adult morbidity or mortality was observed. Genotyping for the *Cre* and *Twist1* transgenes was performed by PCR of DNA isolated from embryonic yolk sacs or 3 weeks postnatal tail clips. The following forward and reverse primer sequences were used: *Cre:* (5'-GCG GTC TGG CAG TAA AAA CTA TC-3' and 5'-GTG AAA CAG CAT TGC TGT CAC TT-3') and *Twist1:* (5'-GCA GTG GTG GAA TGC CTT TA-3' and 5'-TGT GGT ATG GCT GAT TAT GAT CTC-3'). All experiments involving animals were carried out with experimental protocols and procedures reviewed and approved by the Cincinnati Children's Medical Center Biohazard Safety Committee and Institutional Animal Care and Use Committee.

In situ hybridization (ISH) and immunohistochemistry

E12.5 whole embryos, E17.5, P7, and adult mouse hearts were collected and washed in ice cold 1× phosphate buffered saline (PBS) and fixed in 4% paraformaldehyde (PFA) overnight at 4° C. Tissues were subsequently processed for paraffin embedding as previously described (Lincoln et al., 2006) and sectioned at 14 μm for *in situ* hybridization, 5 μm for histological Masson's Trichrome staining, or 7 μm for immunofluorescence. The generation of the *Twist1* antisense RNA probe and ISH were performed as previously described (Chakraborty et al., 2008). For histology, following deparaffinization and hydration through a graded ethanol series (100%, 95%, 75%, 50%), tissues were stained with Masson's trichrome as previously described (Hinton et al., 2006; Levay et al., 2008).

The following antibodies were used for immunofluorescence (IF): Myc (1:400; Cell Signaling, 2272), Phospho-Histone H3 (p-HH3) (1:100; Millipore, 06-570), Ki-67 (1:50; Santa Cruz Biotechnology, 7846), Tbx20 (1:100; Orbigen, PAB 11248), Collagen (Col)2a1 (1:50; Santa Cruz Biotechnology, 52657), Mmp2 (1:50; Abcam, 37150), Mmp13 (1:50; Millipore, MAB 13426), Col1 (1:40; Millipore, AB 765P), Col3 (1:50; Rockland, 600-401-105-0.5), Periostin (Postn) (1:100; Abcam, 14041). Following deparaffinization and hydration, tissue sections for IF were subjected to antigen retrieval in a microwave oven with citrate buffer (10mM Citric acid, 0.05% Tween-20, pH 6.0) for 4.5 minutes at 90% power, followed by 7 minutes at 80% power, and 7 minutes at 70% power and then 2 washes, separately in distilled water and in 1×PBS for 2 minutes each. Tissue sections were incubated with blocking reagent (1% BSA, 0.01% cold water fish skin gelatin, 0.1% Tween- 20 and 0.05% sodium-azide in 1×PBS) for 1 hour at room temperature, followed by overnight incubation at 4° C with primary antibodies with appropriate dilutions in 1×PBS using Coverwell chamber slides (Grace Biolabs). Following incubations, sections were washed in 1×PBS for 10 minutes, incubated with either corresponding Alexa 488 or 568 fluorescent-conjugated secondary antibodies (Molecular Probes, 1:100) for 1 hour, and washed in 1×PBS. Nuclei were stained with ToPro3 (Molecular Probes, 1:1000) for 20 minutes at room temperature. Tissue sections were washed thoroughly

in 1×PBS for 10 minutes and mounted in Vectashield (Vectorlabs). Fluorescent images were captured with Zeiss LSM 510 confocal microscope and LSM version 3.2 SP2 software.

RNA isolation and real-time quantitative RT-PCR (qRT-PCR)

AV valves were isolated from E17.5 embryos or P7 neonates generated from matings of *CAG-CAT-Twist1* females and *Tie2Cre* males. After genotyping, valve tissue from 4–6 embryos or 2–3 neonates was pooled for RNA isolation, and real-time qRT-PCR was performed as previously described (Chakraborty et al., 2008). There was minimal myocardial contamination of the valve RNA samples as indicated by qRT-PCR analysis of the myocardial specific gene, cardiac troponin I (c*TnI*). Forward and reverse primer sequences designed for qRT-PCR are *Tbx20*: (5'-GCA GCA GAG AAC ACC ATC AA-3' and 5'-AAT GAC ACG CGG ATG GTG GGG AAC-3'), *Col2a1:* (5'-GGA AAG TCT GGG GAA AGA GG-3' and 5'-GGA ACC ACT CTC ACC CTT CA-3'), *Mmp2*: (5'-GAT GTC GCC CCT AAA ACA GA-3' and 5'-TGG TGT TCT GGT CAA GGT CA-3'), *Mmp13*: (5' ATC CTG GCC ACC TTC TTC TT-3' and 5'-TTT CTC GGA GCC TGT CAA CT-3'), *Col3a1:* (5'-GCA CAG CAG TCC AAC GTA GA-3' and 5'-TCT CCA AAT GGG ATC TCT GG-3'), *Postn*: (5'-CGA AGG GGA CAG TAT CTC CA-3' and 5'-AGG TCG GTG AAA GTG GTT TG-3'), and *cTnI*: (5'-GAA GCA GGA GAT GGA ACG AG-3' and 5'-TTA AAC TTG CCA CGG AGG TC-3'). The primer sequences for *Col1a1* qRT-PCR were described previously (Chakraborty et al., 2008). All the amplification reactions were performed with 34 cycles of 94°C for 30 seconds; 55°C for 45 seconds; and 72° C for 30 seconds. A standard curve was generated for each experimental primer set with either E17.5 limb or E13.5 whole embryo cDNA, and all values were normalized to ribosomal protein *L7* expression (Hemmerich et al., 1993). The average base-line levels of all the genes relative to *L7* expression in STG AV valves were calculated as described previously (Sengupta et al., 2009). For each gene, normalized expression in STG AV valves is set to 1 and then fold-change is calculated for corresponding DTG AV valves. qRT-PCR results represent three independent experiments (biological n=3) performed in triplicate (technical n=3). Statistical significance of observed differences was determined by Student's *t*-test ($p < 0.01$).

Gene sequence homology analysis

A region containing a canonical Twist E-box (CANNTG) consensus site within the intron I region of the mouse *Col2a1* gene was identified through *Ensembl* alignment of the *Col2a1* gene sequence (ENSMUSG00000022483; Chromosome location 15: 97,805,402-97,835,076). The conserved R1 locus in intron 1 of the *Col2a1* gene was identified by gene homology searches using rVISTA (Frazer et al., 2004; Loots et al., 2002) and Genomatix with MatInspector (Quandt et al., 1995) web-based analytical tools. Sequence alignments demonstrate that the E-box consensus sequence within the murine *Col2a1* intron 1 R1 (CACGTG) is conserved in rat and human *Col2a1* genes.

Chromatin immunoprecipitation (ChIP)

Twist1 binding to chromosomal DNA in vivo was evaluated in mouse E12.5 endocardial cushions dissected from 10–12 wild-type embryos for each immunoprecipitation. Twist1 binding to DNA also was evaluated in MC3T3-E1 (subclone 4) undifferentiated preosteoblasts cultured as previously described, with 4×100 mm tissue culture plates at 90–95% cell confluency used for each immunoprecipitation (Chakraborty et al., 2008). DNA/protein complexes were cross-linked for 10 minutes in formaldehyde (Sigma) at a final concentration of 1%. The fixed cells were lysed and sonicated twice for 5 seconds each with output 5 (Virsonic 60; Virtis) and a 2 minute refractory period. For immunoprecipitation, cell lysates were incubated with an antibody against Twist1 (5 μg; Sigma) and incubated overnight at 4°C with gentle rocking. Immunoprecipitation with normal rabbit IgG was used as a negative control. Chromatin immunoprecipitations were performed according to the manufacturer's instructions

(EZChIP, Upstate), with the exception that protein A-agarose beads were used. The immunoprecipitated and input DNA were subjected to PCR using the following primers: *Col2a1* (R1) 5'- ACC GAA GCC TGG AAA GTG TA-3' and 5'- TCC CCA CCT ACT GTC CAA AC-3' amplifies the murine *Col2a1* regulatory region containing the canonical Twist1 E-box (CACGTG) binding site (R1). Primers used for the negative control region 2 (R2) are: 5'- ATA TTT AGA AAA TCT TGT TA-3' and 5'- AGG GTA GTT GGT GAA ACT AA-3'. PCR amplification reactions were performed with 40 cycles of 94°C for 30 seconds; 55°C for 1.5 minutes; and 72° C for 3 minutes.

Plasmids, Transfection and Dual luciferase assay

The human *Col2a1* (−577/3428) luciferase reporter construct (Peng et al., 2008) was a generous gift from Dr. Mary Goldring, Hospital for Special Surgery, Weill College of Medicine of Cornell University, NY. Site-directed mutagenesis of the Region 1 (R1) E-box was performed in the human *Col2a1* luciferase reporter construct using QuikChange Site-Directed Mutagenesis Kit (Stratagene) according to manufacturer's instructions. The following primers were used for mutagenesis: 5'-GGA TTT TTT TTT CTA CGT TTT TGG GCA CGT TTC C-3' and 5'-GGA AAC GTG CCC AAA AAC GTA GAA AAA AAA ATC C-3'. Successful mutagenesis was verified by sequencing.

Transfections were performed in human embryonic kidney (HEK) 293 cells with FuGENE 6 transfection reagent (Roche) according to manufacturer's protocols. In each experiment, 0.5 μg of either wild-type or mutant luciferase reporter plasmid was cotransfected with 0.1 μg of either pcDNA-Twist1 (Firulli et al., 2007) (kind gift from Tony Firulli, Indiana University School of Medicine) or empty vector (pcDNA3.1). For all experiments, a *Renilla* luciferase reporter pRL-TK (Promega) was co-transfected (0.01 μg) to normalize for transfection efficiency. After 48 hours, cells were washed (1×PBS) and lysed using the passive lysis buffer (Promega), before measuring *firefly* and *Renilla* luciferase activities using the Dual-Luciferase Reporter Assay System (Promega). In each experiment, *firefly* luciferase activity was normalized to *Renilla* luciferase activity. Normalized expression in pcDNA3.1 empty vector control was set to 1 and the fold increase was calculated in the corresponding experimental sample. The average fold change value was calculated from six independent co-transfection experiments performed in triplicate. Statistical significance was determined by Student's *t*-test ($p < 0.01$).

Histology and Immunohistochemistry on Human Valve Tissues

Human aortic valve specimens were obtained from nonsyndromic adult patients with calcific aortic valve disease undergoing aortic valve replacement (8 affected valves) and from age-matched patients at the time of autopsy, who died of noncardiac causes (6 control valves). Patients with a history of infective endocarditis, rheumatic heart disease, or a genetic syndrome were excluded. Control valves with evidence of calcific nodules apparent by von Kossa staining were excluded, however stippled mineralization was observed near the hinge regions in 5/6 control aortic valves, consistent with aging. These studies were approved by the Institutional Review Boards at Cincinnati Children's Medical Center and the University of Cincinnati.

Tissues were processed and analyzed as previously described, and sections (5 μm) were analyzed by Movat's pentachrome or von Kossa histological staining (Hinton et al., 2006) or immunohistochemistry (Snarr et al., 2007), essentially as described previously. The tissue sections were prepared for staining by removal of paraffin wax in xylenes, followed by rehydration through a graded ethanol series into distilled water. For Tbx20, Twist1, and p-HH3 antibody staining, the tissue was then subjected to antigen retrieval using a citric acid antigen unmasking solution (Vector Labs, H-3300), according to manufacturer's instructions, at high temperature and pressure in a standard pressure cooker for 5 minutes (Snarr et al., 2007). For

Col2 antibody staining, the sections were pretreated with 200 units/mL of hyaluronidase (Sigma H3884) in 1× PBS (pH 5.45) at 37°C for 3 hours. The valve tissue sections were incubated with primary antibodies against Twist1 (1:40 dilution, mouse monoclonal; Santa Cruz, sc-81417), p-HH3 (1:350 dilution, rabbit polyclonal; Upstate/Millipore, 06-570), Tbx20 (1:200 dilution, rabbit polyclonal; Orbigen 11248), smooth muscle α-actin (SMA) (1:175 dilution, mouse monoclonal; Sigma 0307), and Col2 (1:25, mouse monoclonal; Developmental Studies Hybridoma Bank, University of Iowa II-II6B3). For colorimetric immunohistochemistry, primary antibodies were detected using the Ultra-sensitive ABC rabbit IgG staining kit (Tbx20, p-HH3) (Thermo Scientific, 32054), or a peroxidase-conjugated goat anti-mouse secondary antibody (SMA, Col2) (Jackson ImmunoResearch 115-035-062). Antibody staining was visualized using the metal enhanced DAB substrate staining kit (Thermo Scientific, 34065). The presence of intact protein in control valve sections was confirmed by robust immunoreactivity with antibodies against SMA and Tbx20. For co-immunofluorescence, the Twist1 primary antibody was detected using a horse anti-mouse biotinylated secondary antibody (from the Vectastain Elite mouse IgG ABC staining kit;Vector Labs, PK-6102) in combination with a streptavidin-conjugated Alexa fluor 488 tertiary antibody (Invitrogen, S11223). The p-HH3 immunoreactivity was detected using an Alexa 568-conjugated goat anti-rabbit secondary antibody (Invitrogen, A11011). Nuclei were stained with ToPro3 (Molecular Probes, 1:1000) in 1× PBS for 10 minutes at room temperature. Fluorescence was visualized using a Zeiss LSM 510 confocal microscope and LSM version 3.2 SP2 software.

Protein isolation and Western Blotting

Protein lysates were isolated from E17.5 whole hearts using ice-cold CelLytic MT tissue lysis buffer (Sigma), containing protease inhibitor mixture (Pierce) and phosphatase inhibitor (Pierce) according to the manufacturer's instructions. Western blots were performed as described previously (Evans-Anderson et al., 2008) except that membranes were incubated with an alkaline phosphatase-conjugated secondary antibody (1:4000; Thermo Scientific). Immunoblots were developed using chemifluorescent detection with the Vistra ECF reagent (Amersham Biosciences) and scanned using a Storm 860 (Amersham Biosciences). Signal intensities were quantified with ImageQuant 5.0 software (GE Healthcare). Twist1 (1:200; Sigma, T6451) and Myc (1:200; Cell Signaling, 2272) primary antibodies were used for immunoblot analyses. GAPDH (1:10,000; Santa Cruz Biotechnology, 25778) antibody reactivity was used as a loading control. Statistical significance was determined by Student's *t*-test ($p < 0.05$).

Valve morphometric analysis

Quantification of mitral valve (MV) and aortic valve (AoV) morphometry was performed on photomicrographs using ImageJ software (NIH). For each time point (E17.5, P7, and 6.5-months), measurements were made on images of 3 sequential tissue sections, stained with Masson's trichrome or Movat's pentachrome, from 4 independent animals of each genotype. Mitral valve leaflet area was measured for the region defined by the distal junction with the chordae tendineae to the insertion into the proximal fibrous continuity, that spans the interventricular septum. The collagen-rich area of the fibrous continuity was also measured independent of valve leaflet area. Valve length was measured from the insertion of the leaflet in the fibrous continuity to the distal tip of the leaflet, excluding the chordae tendineae. Valve thickness was measured at the distal, middle, and proximal (hinge) aspects of the valve leaflets. The distal thickness was measured at the widest aspect of the distal third or tip of the valve, the middle thickness was measured at the thinnest aspect of the middle third of the valve, and the proximal (hinge) thickness was measured at the widest aspect of the hinge of the valve. Aortic valve morphometric analyses were performed as described previously (Hinton et al.,

2008). All the average measurements are reported with standard error of mean (SEM) and were subjected to Student's t-test, with $p < 0.05$ considered significant.

Results

Tie2Cre-mediated Twist1 expression in embryonic and postnatal mouse valves

During normal mouse heart development, *Twist1* mRNA is strongly expressed in E12.5 EC (Fig. 1A), but little to no expression is detected in E17.5 or postnatal day (P)7 AV valve leaflets by ISH (Fig. 1D and G). A conditional transgenic approach was used to achieve persistent expression of Twist1 protein throughout the late stages of valve development and in mature valves in mice. *CAG-CAT-Twist1* transgenic mice express Myc-tagged Twist1 protein in the presence of Cre recombinase (Connerney et al., 2006). These mice were bred with *Tie2Cre* mice (Kisanuki et al., 2001) for expression of Twist1 in endocardial cushion mesenchymal cells and their derivatives in the remodeling and adult valves. For all experiments, single transgenic *CAG-CAT-Twist1* individuals (STG) were directly compared with *CAG-CAT-Twist1;Tie2Cre* double transgenic (DTG) littermates. Induced expression of transgenic Myc-tagged Twist1 protein is apparent in E12.5 AV cushions (Fig. 1C), E17.5 AV valves (Fig. 1F) and in P7 mitral valve (MV) leaflets (Fig. 1I) of DTG animals, compared to no detectable expression in STG littermates (Fig. 1B, E and H). Quantitation of the percent of cells with transgenic Myc-Twist1 expression in DTG animals reveals 49% expression in E12.5 EC, 65% in E17.5 MV, and 39% in P7 MV. Overall, the DTG hearts have a 3.0 fold increase in total Twist1 protein expression at E17.5, compared to littermate STG hearts, as determined by Western Blot (Fig. S1). Therefore the *CAG-CAT-Twist1;Tie2Cre* DTG individuals exhibit persistent Twist1 expression in late embryonic and postnatal heart valves, compared to endogenous Twist1 levels.

Persistent Twist1 expression leads to valve morphogenetic abnormalities associated with increased cell proliferation and Tbx20 expression in heart valves at E17.5

The effects of persistent Twist1 expression on mitral and aortic valve leaflet morphogenesis were quantified (Table 1). Mitral and aortic valve leaflet area, thickness, and length were measured at E17.5 and P7 for DTG animals with persistent Twist1 expression and STG controls. For both MV and AoV leaflets, area, length, and thickness are increased 2–3 fold in DTG versus STG animals at E17.5. Increased MV and AoV leaflet area also is apparent in DTG animals at P7. However the morphogenetic defects are partially resolved after birth with no significant increase in thickness detected in the MV or AoV leaflets in the DTG animals at P7. Together, these studies indicate that persistent Twist1 expression in DTG animals leads to increased MV and AoV leaflet area and thickness at E17.5, but that these morphogenetic abnormalities are less apparent a week after birth.

During normal valve development in mice and humans, proliferation of interstitial cells decreases during remodeling and neonatal stages (Aikawa et al., 2006; Hinton et al., 2006). In contrast, persistent Twist1 expression in the *CAG-CAT-Twist1;Tie2Cre* DTG valves leads to increased cell proliferation relative to STG controls, as detected by immunoreactivity against p-HH3 (Figs. 2 and 3). MV leaflets from E17.5 DTG embryos show an increased number of p-HH3 positive nuclei (Fig. 2B), compared to MV leaflets from littermate STG embryos (Fig. 2A). Quantitation of these results demonstrates that 23.1% of all valve nuclei are p-HH3 positive in E17.5 DTG MV leaflets overexpressing Twist1 compared to 8.3% of nuclei in littermate STG controls (Fig. 2G). Essentially all of the cells with transgenic Twist1 are proliferating, as indicated by co-localization of the cell proliferation marker, Ki-67, and Myc-tagged Twist1 (Fig. 2D, yellow nuclei). Likewise, increased cell proliferation also is detected in E17.5 DTG AoV with persistent Twist1 expression (Fig. 3A–D). In the DTG AoV, 23.2% of the nuclei are p-HH3 positive compared to 7.0% in littermate STG controls (Fig. 3C, D and

G). However, persistent Twist1 expression does not result in increased cell proliferation in P7 DTG MV or AoV leaflets compared to littermate STG controls (Figs. 2E and F; 3E and F). There was no evidence of apoptosis in DTG or STG MV at E17.5 or P7, as determined by TUNEL assay and cleaved caspase-3 immunostaining (Fig. S2). Together, these results demonstrate that increased Twist1 expression promotes cell proliferation in E17.5 remodeling MV and AoV leaflets. However, increased Twist1 expression is not sufficient to induce VIC proliferation after birth.

Tbx20, a T-box transcription factor, was previously identified as a Twist1-responsive gene in chicken primary EC cells in culture (Shelton and Yutzey, 2008). Therefore, expression of Tbx20 was examined in DTG valves with persistent expression of Twist1. Tbx20 expression is increased in E17.5 DTG MV (Fig. 4B) and AoV (Fig. 5B) compared to littermate STG controls (Figs. 4A and 5A). However, Tbx20 expression is not significantly changed in P7 DTG MV (Fig. 4E) and AoV (Fig. 5D) leaflets, compared to littermate STG controls (Fig. 4D and 5C). Expression of *Tbx20* mRNA was quantified by qRT-PCR, demonstrating a 2-fold increase in expression of *Tbx20* mRNA in E17.5 DTG valves overexpressing Twist1 (Fig. 4C). However *Tbx20* mRNA levels are not significantly changed in P7 DTG MV valves (Fig. 4F). Together these data demonstrate that Tbx20 expression is responsive to increased Twist1 expression in E17.5 DTG valves in vivo. However, increased Twist1 expression in DTG valves does not alter Tbx20 expression at P7, consistent with inability of Twist1 to affect cell proliferation postnatally.

Expression of early ECM markers and matrix remodeling enzymes is increased in valves with persistent expression of Twist1

During normal valve development, *Collagen* (*Col*)*2a1* is highly expressed in the immature ECM of the EC and is down-regulated during valve remodeling later in embryogenesis (Chakraborty et al., 2008). Similarly, *Mmp2* and *Mmp13* are preferentially expressed in the primitive EC and are responsive to Twist1 and Tbx20, respectively, in avian EC cultures (Shelton and Yutzey, 2007, 2008). The persistent expression of these EC marker genes was examined in E17.5 DTG valves overexpressing *Twist1*. Persistent Twist1 expression resulted in increased expression of Col2a1 in MV (Fig. 6B) and AoV (Fig. 5F) compared to littermate STG controls (Figs 6A and 5E). In contrast, Twist1 overexpression does not apparently affect Col2a1 expression at P7 in the AoV (Fig. 5G, H), consistent with results obtained for Tbx20 expression (Fig. 5C, D). In E17.5 MV, increased expression of Mmp2 and Mmp13 is detected (Fig. 6D and F) compared to littermate STG controls (Fig. 6C and E). At the transcriptional level, *Col2a1* mRNA expression is increased by 6.3-fold, *Mmp2* by 3.5-fold, and *Mmp13* by 2.6-fold in E17.5 DTG MV overexpressing Twist1 relative to littermate STG controls (Fig. 6G). These data are consistent with Twist1 function in maintaining an ECM characteristic of EC with increased production of primitive ECM markers, including Col2a1 and Mmp13.

Persistent Twist1 expression results in abnormal valve remodeling and morphogenesis

Expression of fibrillar collagen, indicative of normal valve remodeling, was examined in mice with persistent expression of Twist1 in the developing valves. Expression of the matricellular glycoprotein periostin (Postn), that promotes collagen fibrillogenesis in the developing valves and is regulated by Twist1, also was examined (Connerney et al., 2006; Norris et al., 2008; Oshima et al., 2002; Shelton and Yutzey, 2008). In the E17.5 DTG MV with persistent expression of Twist1, expression of Col1 (Fig. 7B) and Col3 (Fig. 7D) is increased compared to littermate STG controls (Figs. 7A, C). Expression of Postn also is increased in E17.5 DTG MV (Fig. 7F) compared to littermate STG controls (Fig. 7E). Likewise, mRNA expression of *Col1a1* is increased by 2.2-fold, *Col3a1* is increased by 3.3-fold, and *Postn* is increased by 2.7-fold in E17.5 DTG MV relative to STG littermates (Fig. 7G). Since fibrillar collagen is the major structural component of the mature valves, the increased expression of Col1, Col3 and

Postn likely contributes to the increased valve thickness and area observed in DTG MV at E17.5 (Table 1). In adults, persistent Twist1 expression leads to less severe valve leaflet abnormalities (Fig. S3 and Supplemental Table 1). However, increased collagen deposition is observed in valve supporting structures and could be an indicator of compromised valve function later in life.

Twist1 binds and activates a *Col2a1* intronic regulatory region

Expression of *Col2a1* is predominant at early stages of EC development (Chakraborty et al., 2008) and also is significantly increased in E17.5 AoV and MV with persistent expression of Twist1 (Figs. 5F and 6B). Therefore the ability of Twist1 to directly regulate *Col2a1* gene expression was examined. A region (R1) containing a conserved canonical Twist E-box (CANNTG) consensus sequence was identified in intron 1 of the *Col2a1* gene (Fig. 8A). Importantly, the mouse R1 E-box sequence (CACGTG) and surrounding nucleotides are conserved in mouse, rat, and human *Col2a1* intron I gene sequences (Fig. 8B). Twist1 binding to the R1 region *in vivo* in mouse E12.5 EC and in cultured MC3T3-E1 pre-osteoblasts that express Twist1 (Chakraborty et al., 2008) was assessed by chromatin immunoprecipitation (ChIP). Crosslinked DNA/protein complexes were isolated directly from dissected murine E12.5 EC or cultured MC3T3-E1 (subclone4) pre-osteoblasts. Immunoprecipitation with Twist1 antisera demonstrated specific binding to R1 sequences in both E12.5 EC and MC3T3 cells (Fig. 8C and D). Immunoprecipitation of R1 was not observed with the IgG negative control. In addition no interaction with Twist1 was observed for an adjacent region R2, which does not include an E-box consensus sequence. Together, these data demonstrate specific binding of Twist1 to the *Col2a1* intronic R1 region in E12.5 EC in vivo and in cultured MC3T3-E1 pre-osteoblast cells.

The ability of Twist1 to activate the *Col2a1* intronic regulatory element was examined in transfection assays performed in cultured HEK 293 cells. A luciferase reporter construct (pGL2B-hCol2a1luc) was obtained that includes human *Col2a1* sequences (−577/+3428), encompassing the promoter, exon 1, and intron 1 regulatory sequences, including the conserved R1 E-box (CACGTG) (Peng et al., 2008). Cotransfection of the wild type (WT) *Col2a1* plasmid with a Twist1 expression plasmid results in an 8.8-fold trans-activation relative to pcDNA empty vector control (Fig. 8E). Site-directed mutagenesis was used to eliminate the E-box consensus sequence of pGL2B-hCol2a1luc(WT) by changing the E-box consensus sequence (**C**ACGT**G**) to (**T**ACGT**T**) in pGL2B-hCol2a1luc(Mut) (* in Fig. 8B). In cotransfection assays, loss of the Twist1 binding site consensus in pGL2B-hCol2a1luc(Mut) essentially eliminates trans-activation by Twist1 (Fig. 8E). Overall, these data demonstrate that the *Col2a1* gene includes a conserved E-box containing regulatory element bound by Twist1 in E12.5 EC and trans-activated by Twist1 in an E-box dependent manner in transfected cells.

Human diseased aortic valves express increased Twist1 and Collagen 2 in areas of ECM disorganization and increased cell proliferation adjacent to calcified nodules

Given that Twist1 affects ECM protein production and promotes proliferation of EC cells in culture and in vivo, we sought to determine if Twist1 expression is induced during human valve pathogenesis. Movat's pentachrome and von Kossa staining was performed on human control and diseased aortic valve tissues in order to identify the layers of stratification (Fig. 9A and B) and areas of calcification (Fig. 9C and D). In all control valves examined (n=6), three distinct layers of ECM were apparent and no calcified nodules were detected (Fig. 9A and C). In contrast, extensive ECM disorganization (Fig. 9B) and nodules of calcification, indicated by dark brown/black von Kossa staining (* in Fig. 9D), are present in the diseased valves (n=8). Twist1 protein expression was examined in diseased and control human aortic valves. Immunofluorescence reveals small clusters of cells with increased expression of Twist1, with 5/8 diseased valves analyzed having Twist1 positive immunostaining (Fig. 9F). The areas of

Twist1 expression are within regions of disorganized ECM and adjacent to focal calcification nodules (* in Fig. 9F). Twist1 expression is not detected in regions of the diseased valves that appear unaffected, nor is Twist1 expression detected in 5/6 control valves analyzed (Fig. 9E). In human diseased aortic valves, Twist1 positive nuclei that also express p-HH3 are detected by co-immunofluorescence, indicating that some Twist1 positive cells are undergoing mitosis (yellow nuclei, Fig. 9F). However, little to no cell proliferation was apparent in the control valves (Fig. 9E). Likewise, increased Col2 protein expression is apparent in diseased aortic valves with increased expression of Twist1 (Fig. 9H) compared to control specimens (Fig. 9G). Together, these results demonstrate overlapping regions of increased Twist1 expression, VIC proliferation, and Col2 protein expression in human aortic valve disease. Overall, these findings are consistent with a mechanism whereby Twist1 activation promotes cell proliferation and Col2 gene expression in aortic valve pathogenesis.

Discussion

Here we demonstrate that Twist1 promotes progenitor cell proliferation and affects expression of several ECM proteins, including the target gene *Col2a1*, during heart valve development in mice. Likewise, increased Twist1 expression is apparent in adult human calcific aortic valve disease. In mice, Tie2Cre-mediated expression of Twist1 promotes cell proliferation and Tbx20 expression during late embryonic heart valve development. Persistent Twist1 expression also results in increased expression of several early ECM markers, including Col2a1, Mmp2 and Mmp13 at this stage (E17.5). In E12.5 EC, Twist1 binds to a conserved Twist1-responsive E-box element present in the *Col2a1* intron 1, supporting direct regulation of gene expression by Twist1. Valve remodeling also is affected by increased Twist1 expression as indicated by thickening of AoV and MV leaflets in addition to dysregulation of mature fibrillar collagen deposition and increased periostin expression at E17.5. In human diseased valves with calcification, increased Twist1, Col2, and cell proliferation are detected in overlapping regions. Co-immunofluorescence provides evidence that a subset of cells expressing Twist1 in the diseased valves is actively proliferating. Overall, these data support a role for Twist1 as a direct regulator of cell proliferation and ECM gene expression in embryonic valve progenitor cells during development. In addition, the detection of increased Twist1 expression in adult valve disease provides initial evidence that Twist1 promotes cell proliferation and Col2 expression during human valve pathogenesis.

A significant reduction in cell proliferation is a feature of late embryonic valve development, and normally little or no cell proliferation is apparent in adult VICs (Aikawa et al., 2006; Hinton et al., 2006; Lincoln et al., 2004). In chicken primary EC cells, Twist1 is necessary and sufficient to promote cell proliferation (Shelton and Yutzey, 2008). In addition, Twist1 promotes Tbx20 expression in avian primary EC explant cultures, and Tbx20 promotes expression of the proto-oncogene *N-myc* in EC and cardiomyocytes (Cai et al., 2005; Shelton and Yutzey, 2007, 2008). Consistent with these data, Tie2Cre-mediated Twist1 overexpression is sufficient to promote cell proliferation and increased Tbx20 expression in E17.5 remodeling valves. However, no significant change is observed in either proliferative indices or Tbx20 expression in postnatal valves overexpressing Twist1. It is possible that Twist1 requires cooperating factors that are absent in postnatal valves in order to promote cell proliferation or that postnatal VICs are refractory to reentering the cell cycle. Together, these findings demonstrate that persistent Twist1 expression is sufficient to prolong the period of cell proliferation in the E17.5 remodeling valve leaflets.

During normal valve development, the primitive, relatively unstructured ECM of the EC remodels into highly organized and stratified ECM of the mature valve leaflets. Valve leaflet remodeling is characterized by the down regulation of early ECM markers and remodeling enzymes and increased expression of mature ECM proteins, including fibrillar collagens and

elastin (Chakraborty et al., 2008; Hinton et al., 2006). Persistent expression of Twist1 results in increased expression of several early ECM markers, including *Col2a1*, *Mmp2*, and *Mmp13*. A direct transcriptional regulatory mechanism is supported by the identification of intronic sequences of the *Col2a1* gene that are bound by endogenous Twist1 in E12.5 EC in vivo and are trans-activated by Twist1 in cultured cells. In addition, Twist1 and Col2 protein expression are induced in overlapping regions of human diseased aortic valves. Since Twist1 expression is normally downregulated during the stages when *Col1a1* and *Col3a1* expression is induced, it is likely that fibrillar collagen gene induction occurs by an indirect mechanism (Chakraborty et al., 2008). Postn expression also is increased with persistent expression of Twist1 in developing mouse valves. In pre-osteoblast cells, Twist1 binds directly to a canonical E-box sequence in the murine *Postn* promoter and trans-activates a *Postn* reporter gene, supporting a direct regulatory mechanism (Oshima et al., 2002). Additional candidate Twist1 downstream target genes identified in mouse valves with persistent Twist1 expression and in avian endocardial cushion cells include *Tbx20*, *Mmp13*, and *cadherin-11*, but Twist1-responsive regulatory elements have not yet been reported for these genes (Shelton and Yutzey, 2007, 2008). Together, these data support Twist1 as a critical transcriptional activator of multiple ECM and remodeling enzyme genes expressed in the mesenchymal EC.

During valve pathogenesis, VICs are activated, apparent in increased cell proliferation, ECM gene induction, and secretion of matrix remodeling enzymes (Schoen, 2008). These properties of activated VIC are shared with valve progenitors of the embryonic EC. The detection of increased Twist1 expression and cell proliferation in human aortic valve disease suggests that Twist1 may influence cell proliferation and VIC activation during disease. Increased Twist1 expression occurs in small clusters of cells in regions displaying ECM disorganization, active cell proliferation, and diseased calcified nodules. Based on our studies in mice, it is unlikely that increased expression of Twist1 alone is sufficient to cause calcific aortic valve disease. However, the observed increase in Twist1 expression in human diseased valves could contribute to cell activation in response to injury, allowing for ECM reorganization and increased cell proliferation. In addition, it is unclear whether Twist1 reactivation during aortic valve disease is part of a protective mechanism for valve repair, or if it has pathologic consequences leading to valve calcification. The origins of activated VICs in valve disease have not been identified, but they could arise from a resident stem cell population or alternatively from extra-cardiac origins, such as mesenchymal or hematopoietic stem cells. There is increasing evidence that regulatory programs active during valve development are reactivated in disease and could be a mechanism for valve homeostasis or regeneration. Therefore, Twist1 function in valve progenitor cell proliferation and ECM gene expression may hold future clinical relevance in human valve disease diagnosis and therapies.

Supplementary Material

Refer to Web version on PubMed Central for supplementary material.

Acknowledgments

We thank Elaine Shelton, Christina Alfieri, Jonathan Cheek, Arunima Sengupta, Michelle Combs, and Mary Horn for technical assistance and scientific discussions. This work was supported by an American Heart Association-Great Rivers Affiliate Post-Doctoral Fellowship (0825627D) to S.C, NIH HL085122 to R.B.H. and NIH HL082716 and HL094319 to K.E.Y.

References

Aikawa E, Whittaker P, Farber M, Mendelson K, Padera RF, Aikawa M, Schoen FJ. Human semilunar cardiac valve remodeling by activated cells from fetus to adult. Circulation 2006;113:1344–1352. [PubMed: 16534030]

Barnes RM, Firulli AB. A twist of insight-the role of Twist-family bHLH factors in development. Int. J. Dev. Biol 2009;53:909–924. [PubMed: 19378251]

Cai CL, Zhou W, Yang L, Bu L, Qyang Y, Zhang X, Li X, Rosenfeld MG, Chen J, Evans S. T-box genes coordinate regional rates of proliferation and regional specification during cardiogenesis. Development 2005;132:2475–2487. [PubMed: 15843407]

Chakraborty S, Cheek J, Sakthivel B, Aronow BJ, Yutzey KE. Shared gene expression profiles in developing heart valves and osteoblast progenitor cells. Physiol. Genomics 2008;35:75–85. [PubMed: 18612084]

Combs MD, Yutzey KE. Heart valve development: Regulatory networks in development and disease. Circ. Res 2009;105:408–421. [PubMed: 19713546]

Connerney J, Andreeva V, Leshem Y, Muentener C, Mercado MA, Spicer DB. Twist1 dimer selection regulates cranial suture patterning and fusion. Dev. Dyn 2006;235:1345–1357. [PubMed: 16502419]

Evans-Anderson HJ, Alfieri CM, Yutzey KE. Regulation of cardiomyocyte proliferation and myocardial growth during development by FOXO transcription factors. Circ. Res 2008;102:686–694. [PubMed: 18218983]

Firulli BA, Redick BA, Conway SJ, Firulli AB. Mutations within helix I of Twist1 result in distinct limb defects and variation of DNA binding affinities. J. Biol. Chem 2007;282:27536–27546. [PubMed: 17652084]

Frazer KA, Pachter L, Poliakov A, Rubin EM, Dubchak I. VISTA: computational tools for comparative genomics. Nucleic Acids Res 2004;32:W273–279. [PubMed: 15215394]

Hemmerich P, von Mikecz A, Neumann F, Sozeri O, Wolff-Vorbeck G, Zoebelein R, Krawinkel U. Structural and functional properties of ribosomal protein L7 from humans and rodents. Nucleic Acids Res 1993;21:223–231. [PubMed: 8441630]

Hinton RB Jr. Alfieri CM, Witt SA, Glascock BJ, Khoury PR, Benson DW, Yutzey KE. Mouse heart valve structure and function: echocardiographic and morphometric analyses from the fetus through the aged adult. Am. J. Physiol. Heart Circ. Physiol 2008;294:H2480–2488. [PubMed: 18390820]

Hinton RB Jr. Lincoln J, Deutsch GH, Osinska H, Manning PB, Benson DW, Yutzey KE. Extracellular matrix remodeling and organization in developing and diseased aortic valves. Circ. Res 2006;98:1431–1438. [PubMed: 16645142]

Kisanuki YY, Hammer RE, Miyazaki J, Williams SC, Richardson JA, Yanagisawa M. Tie2-Cre transgenic mice: a new model for endothelial cell-lineage analysis in vivo. Dev. Biol 2001;230:230–242. [PubMed: 11161575]

Levay AK, Peacock JD, Lu Y, Koch M, Hinton RB Jr. Kadler KE, Lincoln J. Scleraxis is required for cell lineage differentiation and extracellular matrix remodeling during murine heart valve formation in vivo. Circ. Res 2008;103:948–956. [PubMed: 18802027]

Lincoln J, Alfieri CM, Yutzey KE. Development of heart valve leaflets and supporting apparatus in chicken and mouse embryos. Dev. Dyn 2004;230:239–250. [PubMed: 15162503]

Lincoln J, Alfieri CM, Yutzey KE. BMP and FGF regulatory pathways control cell lineage diversification of heart valve precursor cells. Dev. Biol 2006;292:292–302. [PubMed: 16680829]

Loffredo CA. Epidemiology of cardiovascular malformations: prevalence and risk factors. Am. J. Med. Genet 2000;97:319–325. [PubMed: 11376444]

Loots GG, Ovcharenko I, Pachter L, Dubchak I, Rubin EM. rVista for comparative sequence-based discovery of functional transcription factor binding sites. Genome Res 2002;12:832–839. [PubMed: 11997350]

Norris RA, Moreno-Rodriguez R, Sugi Y, Hoffman S, Amos J, Hart MM, Potts JD, Goodwin RL, Markwald RR. Periostin regulates atrioventricular valve maturation. Dev. Biol 2008;316:200–213. [PubMed: 18313657]

Oshima A, Tanabe H, Yan T, Lowe GN, Glackin CA, Kudo A. A novel mechanism for the regulation of osteoblast differentiation: transcription of periostin, a member of the fasciclin I family, is regulated by the bHLH transcription factor, twist. J. Cell. Biochem 2002;86:792–804. [PubMed: 12210745]

Peng H, Tan L, Osaki M, Zhan Y, Ijiri K, Tsuchimochi K, Otero M, Wang H, Choy BK, Grall FT, Gu X, Libermann TA, Oettgen P, Goldring MB. ESE-1 is a potent repressor of Type II collagen gene (COL2A1) transcription in human chondrocytes. J. Cell. Physiol 2008;215:562–573. [PubMed: 18044710]

Quandt K, Fech K, Karas H, Wingender E, Werner T. MatInd and MatInspector: new fast and versatile tools for detection of consensus matches in nucleotide sequence data. Nucleic Acids Res 1995;23:4878–4884. [PubMed: 8532532]

Rabkin E, Aikawa M, Stone JR, Fukumoto Y, Libby P, Schoen FJ. Activated interstitial myofibroblasts express catabolic enzymes and mediate matrix remodeling in myxomatous heart valves. Circulation 2001;104:2525–2532. [PubMed: 11714645]

Rabkin-Aikawa E, Farber M, Aikawa M, Schoen FJ. Dynamic and reversible changes in interstitial cell phenotype during remodeling of cardiac valves. J. Heart Valve Disease 2004;13:841–847. [PubMed: 15473488]

Reardon W, Winter RM. Saethre-Chotzen syndrome. J. Med. Genet 1994;31:393–396. [PubMed: 8064818]

Roberts WC, Ko JM. Frequency by decades of unicuspid, bicuspid, and tricuspid aortic valves in adults having isolated aortic valve replacement for aortic stenosis, with or without associated aortic regurgitation. Circulation 2005;111:920–925. [PubMed: 15710758]

Schoen FJ. Evolving concepts of cardiac valve dynamics: the continuum of development, functional structure, pathobiology, and tissue engineering. Circulation 2008;118:1864–1880. [PubMed: 18955677]

Sengupta A, Molkentin JD, Yutzey KE. FoxO transcription factors promote autophagy in cardiomyocytes. J. Biol. Chem 2009;284:28319–28331. [PubMed: 19696026]

Shelton EL, Yutzey KE. Tbx20 regulation of endocardial cushion cell proliferation and extracellular matrix gene expression. Dev. Biol 2007;302:376–388. [PubMed: 17064679]

Shelton EL, Yutzey KE. Twist1 function in endocardial cushion cell proliferation, migration, and differentiation during heart valve development. Dev. Biol 2008;317:282–295. [PubMed: 18353304]

Snarr BS, O'Neal JL, Chintalapudi MR, Wirrig EE, Phelps AL, Kubalak SW, Wessels A. Isl1 expression at the venous pole identifies a novel role for the second heart field in cardiac development. Circ. Res 2007;101:971–974. [PubMed: 17947796]

Yang J, Mani SA, Donaher JL, Ramaswamy S, Itzykson RA, Come C, Savagner P, Gitelman I, Richardson A, Weinberg RA. Twist, a master regulator of morphogenesis, plays an essential role in tumor metastasis. Cell 2004;117:927–939. [PubMed: 15210113]

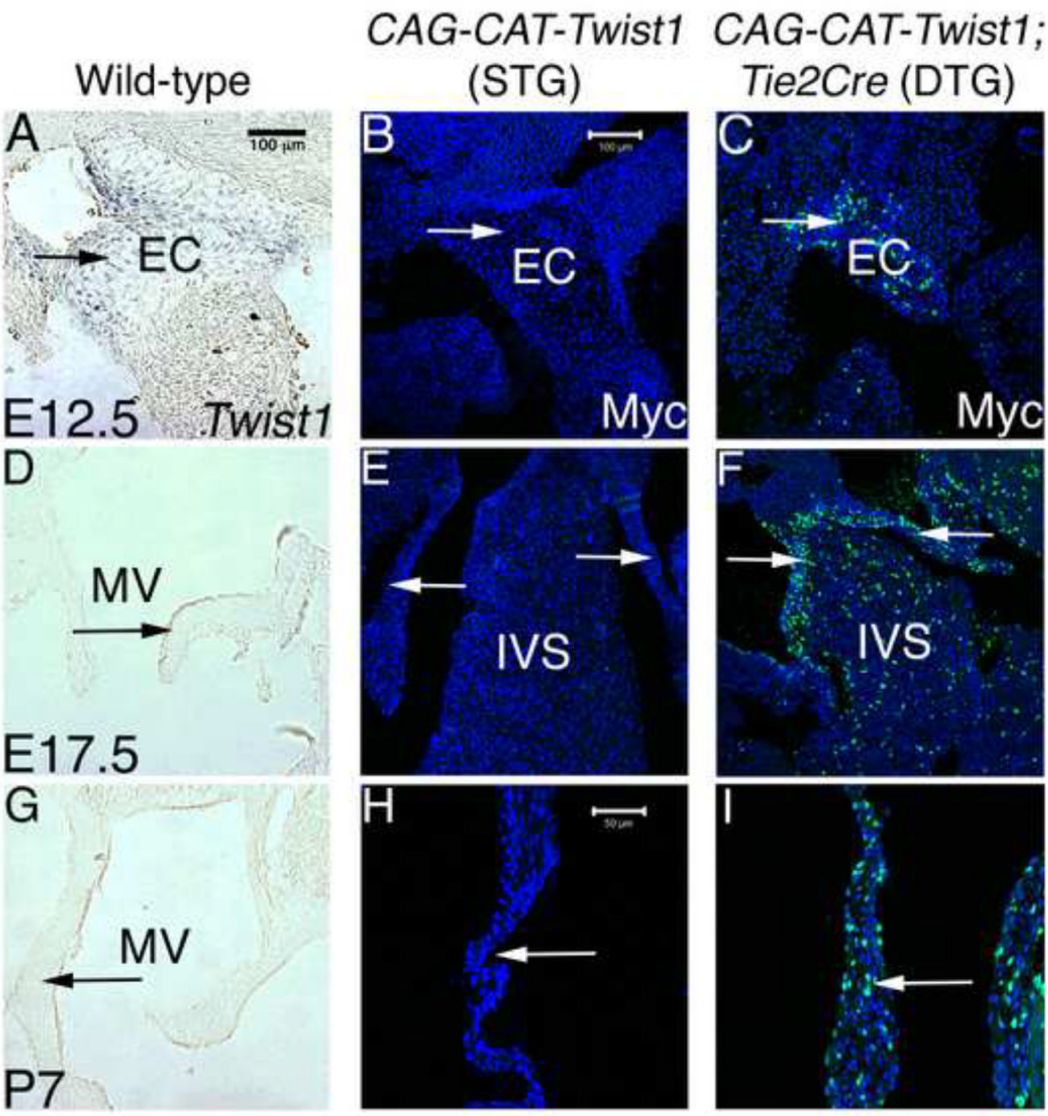

Figure 1. Ectopic Twist1 is expressed in late embryonic and postnatal AV valves in *CAG-CAT-Twist1;Tie2Cre* transgenic mice

In situ hybridization for mouse *Twist1* reveals endogenous expression indicated by arrows in (A) E12 5 endocardial cushion (EC) cells, but not in E17.5 (D) or P7 (G) mitral valve leaflets. Tie2Cre-mediated expression of Myc-tagged Twist1 is apparent by immunofluorescence (arrows, green nuclei) throughout the EC at E12.5 (C), in E17.5 AV valves (F), and P7 MV leaflets (I) in *CAG-CAT-Twist1;Tie2Cre* (DTG) mice. *CAG-CAT-Twist1* (STG) littermates show no immunoreactivity against the Myc antibody at E12.5 (B), E17.5 (E), or P7 (H). Cell nuclei are stained blue with ToPro3. The interventricular septum (IVS) is indicated. Similar results were obtained for n=4 individuals for each genotype. Scale bar represents 100 μm for A–G and 50 μm for H and I.

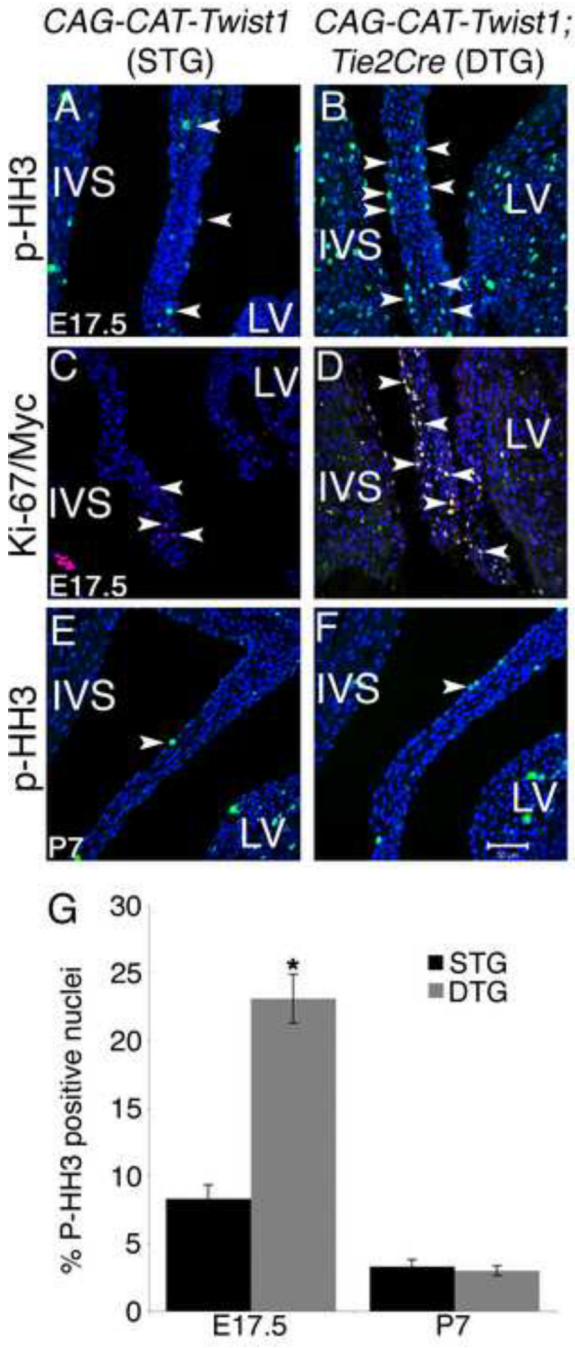

Figure 2. Twist1 promotes increased cell proliferation in late embryonic but not in postnatal AV valve leaflets

Increased cell proliferation as indicated by p-HH3 immunofluorescence (green nuclei, arrowheads) is apparent in developing valves of E17.5 DTG embryos (B) relative to STG littermates (A). The proliferation marker, Ki-67 (red) is colocalized with Myc-tagged (green) Twist1 protein in E17.5 DTG valve leaflets, as indicated by yellow nuclei and arrowheads in D, compared to control STG leaflets (arrowheads in C). Comparable p-HH3 immunoreactivity is observed in P7 DTG MV leaflets (F) relative to the littermate STG controls (E). (G) p-HH3 reactivity was quantified as the percent of total nuclei positive for pHH3 in 3 separate sections for 4 individuals of each genotype. The percent p-HH3 positive nuclei is increased in E17.5

DTG (23.1%) compared to STG (8.3%) valves. In contrast, similar levels of proliferation are apparent at P7, as indicated by percent p-HH3 positive nuclei in P7 DTG mitral valve leaflets (3.0%) compared to littermate STG controls (3.3%). Statistical significance is determined by Student's *t*-test, where * denotes $p < 0.01$. Scale bar represents 50 μm.

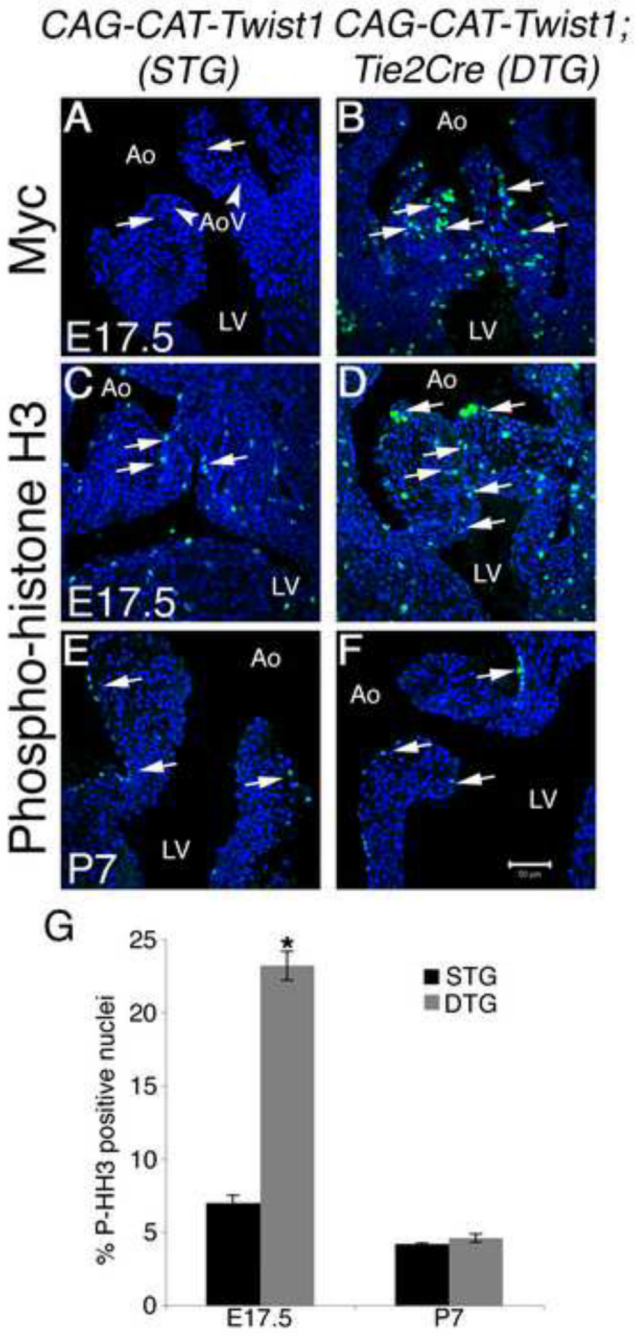

Figure 3. Cell proliferation is increased in E17.5 *CAG-CAT-Twist1;Tie2Cre* (DTG) aortic valves with persistent Twist1 expression

(A, B) Tie2Cre-mediated expression of Myc-tagged Twist1 (green nuclei) in *CAG-CAT-Twist1;Tie2Cre* mice is detected throughout the E17.5 aortic valve leaflets (arrows in B). In contrast, comparable heart sections from littermate STG embryos show no immunoreactivity against the Myc epitope at E17.5 (arrows in A). (C, D) Persistent Twist1 expression in E17.5 aortic valves leads to increased cell proliferation in *CAG-CAT-Twist1;Tie2Cre* DTG embryos, as indicated by p-HH3 antibody reactivity (green nuclei indicated by arrows in D), compared to fewer p-HH3 positive green nuclei in STG littermates (arrows in C). (G) p-HH3 reactivity was quantified in 3 separate sections from 3 individuals of each genotype by cell counts of p-

HH3 positive nuclei/total nuclei. Increased p-HH3 positive nuclei (23.2%) were observed in E17.5 DTG compared to 7.0% in STG valves. (E, F) In contrast, similar levels of proliferation were detected in DTG and STG aortic valve leaflets at P7, as indicated by percent p-HH3 positive nuclei in P7 DTG aortic valve leaflets (4.6%) compared to littermate STG controls (4.2%). Cell nuclei are stained blue with ToPro3. Statistical significance is determined by Student's *t*-test, where * denotes $p < 0.01$. Scale bar represents 50 μm. Ao = aorta; AoV = aortic valve leaflets, LV = left ventricle.

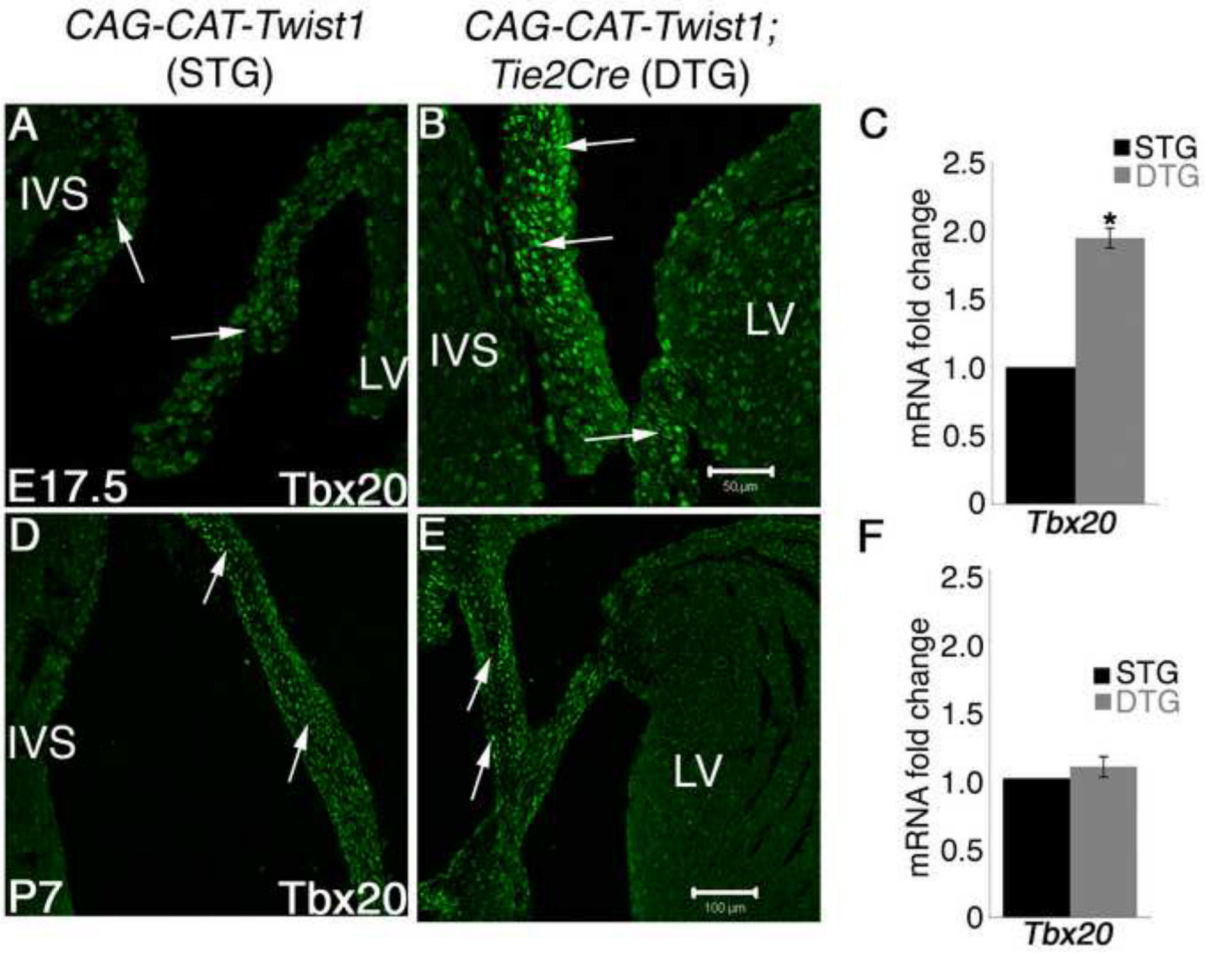

Figure 4. Twist1 promotes Tbx20 expression in late embryonic AV valves

Tbx20 expression, as indicated by immunofluorescence (green), is increased in E17.5 DTG MV leaflets (B, arrows) compared to littermate STG controls (A, arrows). The left ventricle (LV) and interventricular septum (IVS) are indicated. (C) qRT-PCR analysis reveals a 2-fold up-regulation of *Tbx20* mRNA in E17.5 DTG valves relative to littermate STG controls. Tbx20 expression is comparable in P7 DTG MV leaflets (E, arrows) and littermate STG controls (D, arrows) as detected by immunofluorescence and qRT-PCR (F). Normalized *Tbx20* expression in E17.5 or P7 STG AV valves is set to 1 and then fold-change is calculated for corresponding DTG AV valves. The average base-line levels of *Tbx20* relative to *L7* expression in STG AV valves are 1.14 at E17.5 and 2.03 in P7, respectively. The average fold increase is depicted, where n = 3 and error bars represent SEM. Statistical significance is determined by Student's *t*-test, where * denotes $p < 0.05$. Scale bar represents 50 μm (A, B) and 100 μm (D, E).

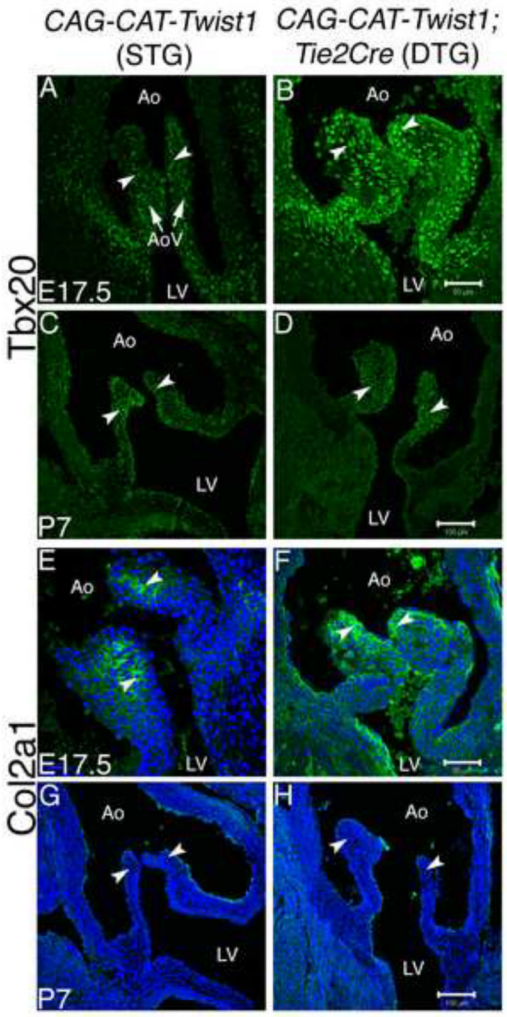

Figure 5. Twist1 promotes Tbx20 and Col2a1 expression in late embryonic but not in postnatal aortic valves

(A, B) Tbx20 expression as indicated by immunofluorescence (green) is increased in E17.5 DTG aortic valves (B, arrowheads) compared to littermate STG controls (A, arrowheads). Likewise, increased expression of Col2a1 is detected in E17.5 DTG aortic valves (F, arrowheads) compared to littermate STG controls (E, arrowheads). Expression of Tbx20 (C, D arrowheads) and Col2a1 (G, H arrowheads) proteins is similar for STG and DTG animals at P7. (E–H) Cell nuclei are stained blue with ToPro3. Scale bar represents 50 μm for A, B, E and F; and 100 μm for C, D, G and H. Ao = aorta; AoV = aortic valve, LV = left ventricle.

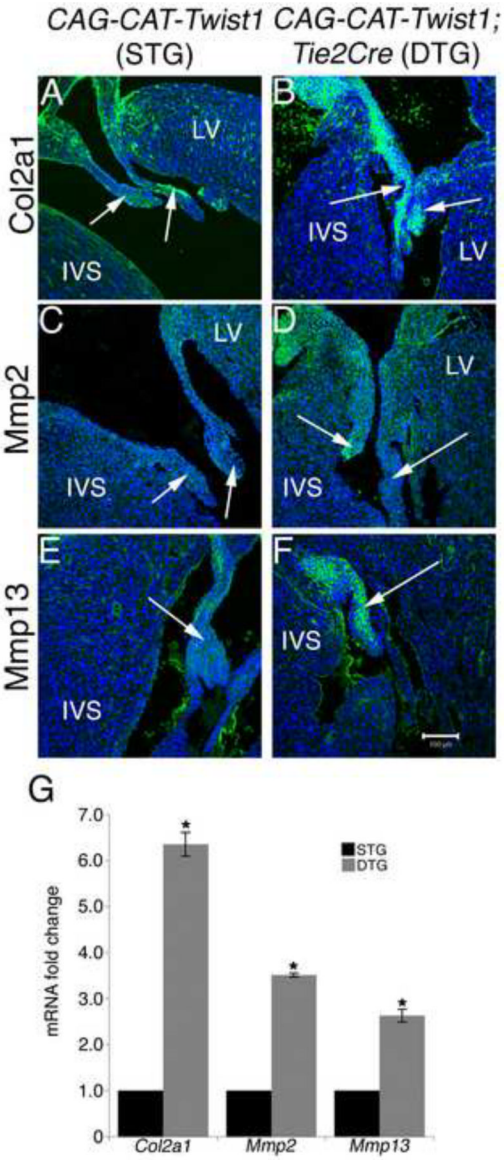

Figure 6. Expression of early ECM markers characteristic of endocardial cushions is increased in *CAG-CAT-Twist1;Tie2Cre* mouse valves at E17.5

Expression of ECM proteins (A, B) Col2a1, (C, D) Mmp2 and (E, F) Mmp13 was detected by immunofluorescence (green, arrows) in E17.5 DTG mitral valves and littermate STG controls. (G) qRT-PCR was used to determine mRNA expression levels of *Col2a1*, *Mmp2* and *Mmp13* (n=3). The average level of expression for each gene in E17.5 STG AV valves is set to 1 and the fold changes are calculated for the E17.5 DTG AV valves. The average base-line levels of expression relative to the *L7* normalization gene are *Col2a1* (3.13), *Mmp2* (2.98), and *Mmp13* (0.30) in E17.5 STG AV valves. Statistical significance is determined by Student's *t*-test, where * denotes $p < 0.05$. Scale bar represents 100 μm. IVS = interventricular septum; LV = left ventricle.

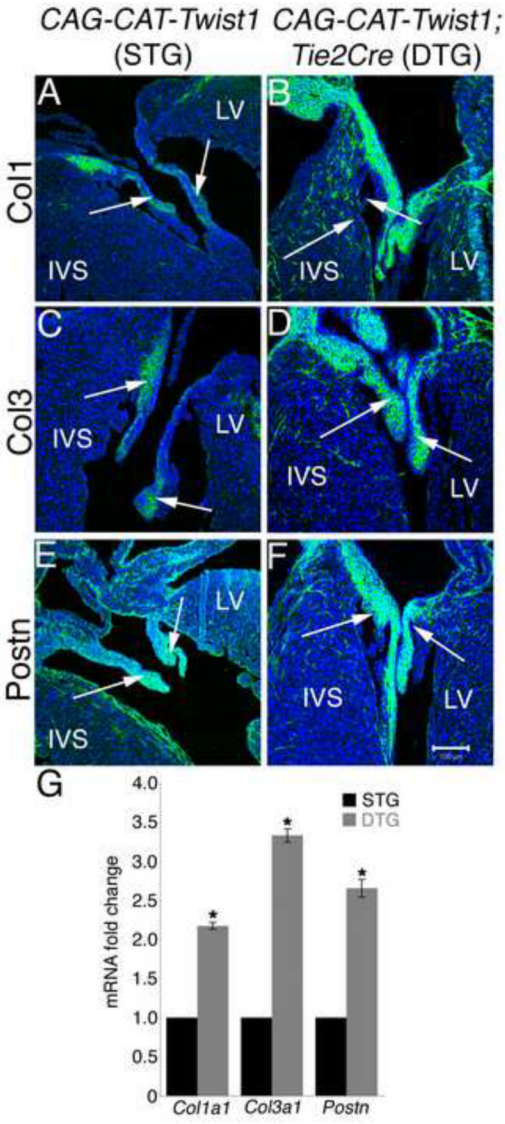

Figure 7. Heart valve ECM remodeling, as indicated by expression of fibrillar collagens and periostin, is abnormal in *CAG-CAT-Twist1;Tie2Cre* mice at E17.5

Expression of ECM proteins (A, B) Col1, (C, D) Col3, and (E, F) Postn, was detected by immunofluorescence (green, arrows) in E17.5 DTG mitral valves and corresponding littermate STG controls. (G) qRT-PCR demonstrates that *Col1a1*, *Col3a1*, and *Postn* mRNA levels are increased in DTG versus STG (n=3) E17.5 embryos as described for Figure 4. The average base-line levels of *Col1a1*, *Col3a1*, and *Postn* are 1.04, 3.12, and 1.52 relative to *L7* expression in E17.5 AV valves, respectively. Statistical significance is determined by Student's *t*- test, where * denotes $p < 0.05$. Scale bar represents 100 μm. IVS = interventricular septum; LV = left ventricle.

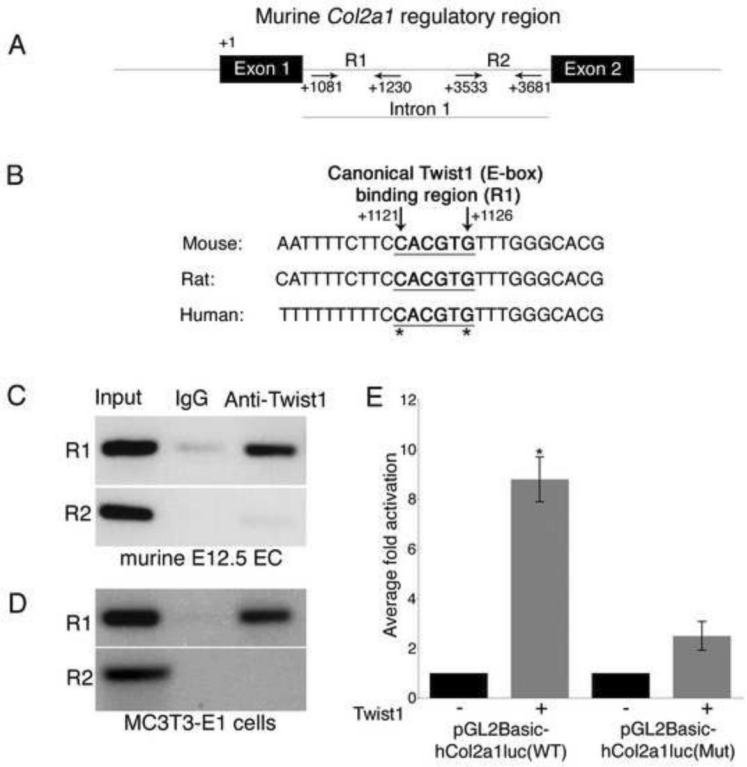

Figure 8. Twist1 binds directly and trans-activates a *Col2a1* intronic regulatory region

(A) The mouse *Col2a1* gene contains a conserved E-box sequence in region R1. Arrows indicate PCR primer sequences for amplification of R1 and of a negative control region 2 (R2), that does not contain an E-box consensus sequence. (B) The murine R1 E-box consensus sequence (CACGTG) is conserved in rat and human *Col2a1* genes. E-box consensus nucleotides mutated in R1 for transfection studies are indicated by *. (C–D) ChIP assays demonstrate that Twist1 binds *Col2a1* R1, but not R2 sequences, in mouse E12.5 EC (C) and MC3T3-E1 cells (D). (E) Cotransfection experiments performed in HEK293 cells demonstrate that human *Col2a1* (−577 to +3428) sequences linked to a pGL2-Basic reporter are trans-activated by Twist1 (8.8-fold). Mutagenesis of the conserved R1 E-box leads to reduced trans-activation of *Col2a1* regulatory sequences by Twist1. Trans-activation is represented as fold-change relative to the pcDNA empty vector control. Data are shown for a representative experiment (from n=6) performed in triplicate. Statistical significance is determined by Student's *t*-test, where * denotes $p < 0.01$.

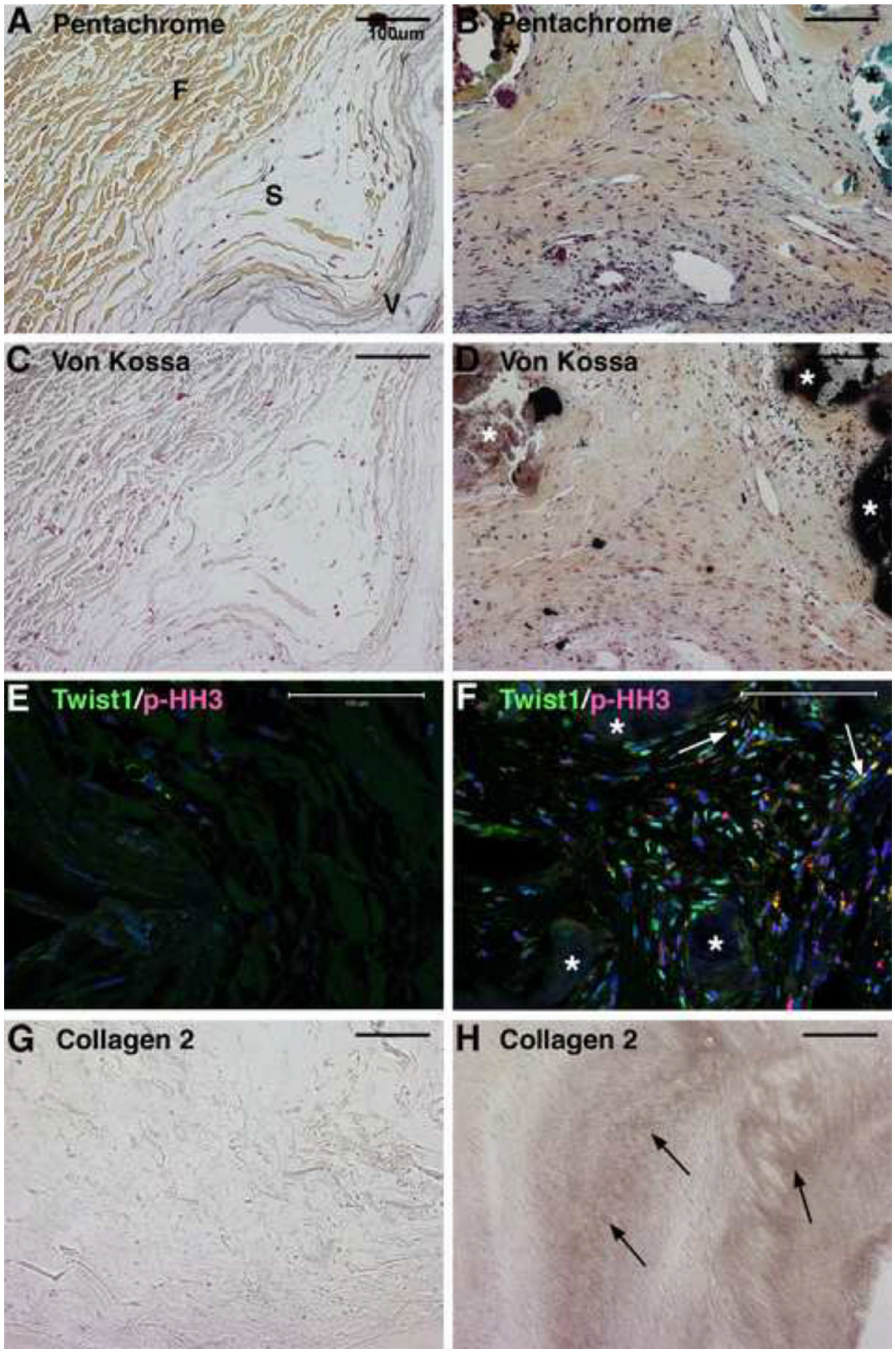

Figure 9. Twist1 and Collagen 2 expression is upregulated and cell proliferation is increased in human aortic valve disease

(A, C, E, G) Human control aortic valve tissue collected at the time of autopsy. (B, D, F, H) Human diseased aortic valve tissue obtained following valve replacement surgery. (A) Movat's Pentachrome staining of normal human aortic valve tissue delineates Fibrosa (F), Spongiosa (S), and Ventricularis (V) layers. (B) Pentachrome staining of the diseased human aortic valve demonstrates disorganized stratification. The presence of calcification in the diseased human valve is apparent by von Kossa staining (D, black staining indicated by white *), in comparison to the control tissue (C). Control and diseased tissues were immunostained for Twist1 (E, F, green nuclei) and p-HH3 (E, F, red nuclei). Increased expression of Twist1 (F, green nuclei)

and p-HH3 (F, red nuclei) is observed in the diseased human aortic valve tissues adjacent to areas of calcification (indicated by *) and co-localization is demonstrated by yellow nuclei (F, white arrows). In contrast, Twist1 and p-HH3 immunoreactivity is not apparent in control aortic valve tissue (E). Collagen 2 immunostaining (brown) also is increased in diseased aortic valves (arrows in H) relative to controls (G). 5/8 diseased valves analyzed have Twist1 positive immunostaining, while 1/6 control valves have Twist1 positive immunostaining. Scale bar represents 100 μm.

Table 1

Morphometric analyses of mitral and aortic valve leaflets from E17.5 and P7 animals. Mean values for at least n=3 individuals per group are indicated ± S.E.M.

Age	Mitral valve measurement (mm)	*CAG-CAT-Twist1* (STG)	*CAG-CAT-Twist1*; *Tie2Cre* (DTG)
E17.5	Area mm^2 (leaflet)	43.20 ± 1.28	145.47 ± 1.09*
	Length	0.82 ± 0.01	1.03 ± 0.006*
	Thickness at distal region	0.08 ± 0.001	0.18 ± 0.004*
	Thickness at middle region	0.05 ± 0.001	0.14 ± 0.002*
	Thickness at hinge region	0.07 ± 0.002	0.27 ± 0.009*
P7	Area (leaflet)	33.47 ± 0.08	57.20 ± 0.44*
	Area (fibrous continuity)	4.17 ± 0.22	3.80 ± 0.22
	Length	0.83 ± 0.002	1.02 ± 0.005*
	Thickness at distal region	0.03 ± 0.001	0.03 ± 0.002
	Thickness at middle region	0.06 ± 0.001	0.03 ± 0.003
	Thickness at hinge region	0.07 ± 0.001	0.10 ± 0.002

Age	Aortic valve measurement (mm)	*CAG-CAT-Twist1* (STG)	*CAG-CAT-Twist1*; *Tie2Cre* (DTG)
E17.5	Area mm^2 (leaflet)	10.18 ± 0.23	20.48 ± 1.06*
	Length	0.26 ± 0.03	0.41 ± 0.02*
	Thickness at distal region	0.02 ± 0.001	0.04 ± 0.006
	Thickness at middle region	0.03 ± 0.002	0.08 ± 0.006*
	Thickness at hinge region	0.04 ± 0.002	0.05 ± 0.004
P7	Area (leaflet)	12.53 ± 0.52	20.31 ± 1.32*
	Area (annulus)	4.68 ± 0.34	13.02 ± 0.35*
	Length	0.31 ± 0.01	0.32 ± 0.02
	Thickness at distal region	0.03 ± 0.03	0.02 ± 0.009
	Thickness at middle region	0.01 ± 0.01	0.02 ± 0.006
	Thickness at hinge region	0.02 ± 0.02	0.03 ± 0.012

* indicates statistical significance as determined by Student's t-test $p < 0.05$.